RSC Advances

PAPER

View Article Online
View Journal | View Issue

Cite this: *RSC Adv.*, 2023, **13**, 29802

Chemical reactivity of the tryptophan/acetone/DMSO triad system and its potential applications in nanomaterial synthesis†

Chun-Yi Huang, Hsiao-Wei Liao and Teh-Min Hu *

Received 27th September 2023
Accepted 6th October 2023

DOI: 10.1039/d3ra06596k

rsc.li/rsc-advances

Previously, we reported a novel browning reaction of amino acids and proteins in an organic solvent mixture composed of dimethyl sulfoxide (DMSO) and acetone. The reaction proceeds under surprisingly mild conditions, requiring no heating or additional reactants or catalysts. This present study aimed to investigate the chemical reactivity of the triad reaction system of L-tryptophan/aectone/DMSO. We demonstrated that, in DMSO, L-tryptophan initially catalyzed the self-aldol condensation of acetone, resulting in the formation of mesityl oxide (MO). Furthermore, we showed that the three-component system evolved into a diverse chemical space, producing various indole derivatives with aldehyde or ketone functional groups that exhibited self-assembling and nanoparticle-forming capabilities. We highlight the potential applications in nanomaterial synthesis.

1. Introduction

The Maillard reaction, also known as the browning reaction, was first introduced by the French chemist Louis Camille Maillard in 1912.[1] It is a complex series of chemical reactions that occur when a reducing sugar reacts with an amino acid, resulting in the formation of a diverse range of compounds and pigments.[2–8] In our recent investigation,[9] we made an unexpected discovery: intense browning of L-tryptophan in a solvent mixture composed of two commonly used solvents, acetone and dimethyl sulfoxide (DMSO). This novel browning reaction exhibits several distinctive features when compared to the conventional browning reaction. Firstly, it takes place in a nonaqueous environment at room temperature. Secondly, it does not necessitate the presence of a reducing sugar. Thirdly, the volume ratio of acetone to DMSO significantly impacts the overall reactivity, specifically the extent of browning. Thus, simply dissolving L-tryptophan in the acetone/DMSO cosolvent and allowing the solution to stand undisturbed at room temperature results in the generation of a brown solution within hours. The intriguing aspect lies in understanding how such a straightforward mixture exhibits such reactivity and the underlying complexity involved.

In 2000, List *et al.*[10] made a groundbreaking discovery, demonstrating the catalytic potential of L-proline (30 mol%) in asymmetric aldol reactions between acetone and aldehydes in anhydrous DMSO at room temperature. This pivotal finding marked the emergence of a new era in organocatalysis, leading to extensive research over the past two decades on metal-free amino acid-based catalysis.[11–19] The significant contributions of this field to various scientific and technological domains were acknowledged through the 2021 Nobel Prize in Chemistry. In contrast, our previous study revealed limited browning reactivity of L-proline in acetone/DMSO, while L-tryptophan exhibited the highest browning potential within our specific system. As the largest amino acid, L-tryptophan is believed to be the last to evolve among the 20 canonical amino acids due to its structural complexity.[20] The indole ring and hydrophobic characteristics of L-tryptophan play crucial roles in stabilizing peptides and proteins.[20,21] L-tryptophan has also demonstrated its catalytic ability in the direct aldol reaction between cyclic ketones and aromatic aldehydes in water at room temperature. This reaction forms a two-phase system comprising dispersed hydrophobic particles of L-tryptophan in water, resembling heterogeneous "on water" catalysis.[22,23]

Pertinent to our present investigation, a limited number of studies have investigated the browning reactivity of L-tryptophan in aqueous media in the presence of reducing sugars and under conditions of vigorous heating, typically associated with the conventional Maillard reaction.[24–28] Moreover, compounds isolated from the aqueous Maillard reaction of L-tryptophan have exhibited notable biological activities.[29–31] To summarize, while L-tryptophan can serve as an effective catalyst in aldol reactions, this capability is observed exclusively in heterogeneous aqueous solutions. Furthermore, in water, L-tryptophan can also act as a stoichiometric reactant in the conventional Maillard reaction. Hence, observing the browning of L-

Department of Pharmacy, College of Pharmaceutical Sciences, National Yang Ming Chiao Tung University, 112304, Taipei, Taiwan. E-mail: tehmin@nycu.edu.tw

† Electronic supplementary information (ESI) available: Experimental and additional tables and figures for related components. See DOI: https://doi.org/10.1039/d3ra06596k

tryptophan in a simple solvent mixture at room temperature is unexpected.

In this study, our primary objective was to gain a deeper understanding of the chemical processes involved in the browning of L-tryptophan in a binary solvent mixture of acetone and DMSO. We were particularly intrigued by the transformation of a simple, colorless solvent system consisting of L-tryptophan, acetone, and DMSO into a complex network of reactions, leading to the production of brown species. Through comprehensive liquid chromatography and mass spectrophotometry-based measurements, we aimed to provide an initial insight into the chemical landscape occupied by the components of this reaction system. Our findings demonstrate that L-tryptophan acts as both an organocatalyst and a stoichiometric reactant in the acetone/DMSO environment. Specifically, L-tryptophan catalyzes the direct aldol condensation of acetone, forming reactive intermediates that subsequently react with and consume L-tryptophan. Additionally, we present preliminary evidence that the newly discovered chemical space encompasses diverse hydrophobic compounds capable of self-assembling into nanoparticles through a nanoprecipitation mechanism. This investigation into self-assembly highlights the potential for synthesizing innovative functional nanomaterials with wide-ranging applications.

2. Experimental section

2.1 General information

All compounds and solvents were purchased from vendors and used without additional purification. Deionized water was obtained using the ELGA PURELAB Ultra water purification system.

2.2 L-Tryptophan browning in acetone/DMSO

Solutions of L-tryptophan at various concentrations (2.5, 5, 7.5, and 10 mg mL^{-1}) were prepared using a solvent mixture of 9 mL of DMSO and 1 mL of acetone. The reaction was allowed to stand at room temperature and monitored over a period of 7 days by recording UV-Vis spectra at different time points using a Tecan Spark multimode microplate reader. Prior to measurements, all samples were appropriately diluted to a suitable concentration. The presented UV-Vis spectra have been adjusted based on the sample's dilution factor.

2.3 Kinetic study

L-Tryptophan (50 mg) was dissolved in the solvent mixture consisting of 4.5 mL of DMSO and 0.5 mL of acetone to obtain a sample solution of 10 mg mL^{-1}. The solution was left standing at room temperature and monitored over a period of 12 days. At predetermined sampling intervals, a 50 μL aliquot of the solution was taken and diluted with 950 μL of deionized water. It has been previously confirmed that adding water to the sample solution completely stops the reaction. The diluted samples were stored at −80 °C until analysis using a validated high-performance liquid chromatography with diode-array detection (HPLC-DAD) method (see ESI† for LC conditions) for L-tryptophan, acetone, mesityl oxide (MO) (Table S1†). Each sampling time was performed in triplicate ($n = 3$). Kinetic data fitting was conducted using GraphPad Prism7.

2.4 Reactivity under different reaction conditions and comparison among amino acids

The influence of solvent conditions on the production of MO was investigated using a 10 mg mL^{-1} solution of L-tryptophan. The amino acid was dissolved in a 20 mL glass vial containing either 10 mL of a single solvent (DMSO or acetone) or a solvent mixture of DMSO and acetone. The solutions were tightly capped and left undisturbed at room temperature for 24 hours. The resulting amount of MO generated was analysed using the HPLC-DAD method described above. Prior to measurement, the samples were diluted 20 times by combining 50 μL of the sample solution with 950 μL of deionized water. For the binary solvent system (DMSO/acetone, v/v) with 10 mg mL^{-1} of L-tryptophan, the system was examined at various acetone percentages ranging from 5–15% v/v. In the case of the binary solvent system (DMSO/acetone) with a ratio of 9 : 1 (v/v), the reactivity of the reaction system was also assessed at various concentrations of L-tryptophan (2.5, 5, and 7.5 mg mL^{-1}). For the remaining 19 amino acids, the reaction was carried out using saturated solutions of each amino acid at a concentration of 10 mg mL^{-1} in the same binary solvent system (DMSO/acetone) with a ratio of 9 : 1 (v/v). All reaction conditions were kept consistent with those used for L-tryptophan. Each experiment was performed in triplicate ($n = 3$).

2.5 Identification of MO

L-Tryptophan (50 mg) was dissolved in a 5 mL solvent mixture consisting of 90% (v/v) DMSO and 10% (v/v) of acetone or deuterated acetone (acetone-d_6). The reaction was conducted at 25 °C, controlled by a water bath system, for 3 hours. Subsequently, the samples were diluted to a suitable concentration with deionized water and analysed using an ultra-high-performance liquid chromatography (UHPLC) coupled with ultra-high-resolution time-of-flight mass spectrometry (UHR-TOF-MS) (see ESI† for details). The MS spectra data were extracted using Bruker software Data Analysis 4.1.

2.6 Untargeted profiling of the browning solution and standards confirmation

L-Tryptophan (50 mg) was dissolved in a 5 mL solvent mixture consisting of 90% (v/v) DMSO and 10% (v/v) of acetone. The reaction was conducted at 25 °C, controlled by a water bath system, for 6 days. Subsequently, the samples were diluted to a suitable concentration with deionized water and analysed using an ultra-performance liquid chromatography system coupled with time-of-flight mass spectrometry (UPLC-TOF-MS) (see ESI† for details). The MS spectra data were extracted using Progenesis software for analysis. In order to detect the presence of tryptamine and indole-3-acetaldehyde in the sample, standard of each compound was dissolved in a solvent mixture comprising 90% (v/v) DMSO and 10% (v/v) acetone. The sample was then diluted to a concentration of 1 μg mL^{-1} using

deionized water and analysed using the same UPLC-TOF-MS system and parameters, except for the gradient conditions (see ESI†).

2.7 Preparing and characterizing nanoparticles

L-Tryptophan (200 mg) was dissolved in a solvent mixture containing 18 mL of DMSO and 2 mL of acetone to create a 10 mg mL^{-1} solution of L-tryptophan. After allowing the reaction to proceed without stirring at 25 °C (controlled by a water bath system) for 6 days, 2 mL of organic phase was taken and added dropwise to a 10 mL aqueous solution containing 0.01% bovine serum albumin (BSA). The mixing procedure was completed within 15 seconds using an S1 pipette filler (Thermo Fisher Scientific Inc., Waltham, USA). The resulting mixture was magnetically stirred (300 rpm) for 30 seconds at room temperature, followed by aging for 1 hour in a water bath at 25 °C. The aged solution was then centrifuged at 10 000*g* for 20 minutes to separate the nanoparticles from the supernatant. The particle pellet was subsequently washed twice by repeating the redispersion–centrifugation cycle using a 0.01% BSA aqueous solution. The morphology of the washed nanoparticles was examined by JEOL JEM-1400plus transmission electron microscopy and JEOL JSM-7600F scanning electron microscopy. The zeta potential was measured by dynamic light scattering (DLS) using the Zetasizer Nano (Malvern, Worcestershire, UK). Each 1 mL sample was measured 3 times, and the mean value was recorded.

3. Results and discussion

Fig. 1 reveals that L-tryptophan undergoes rapid and intense browning in acetone/DMSO at room temperature. The observed colour changes correspond to spectral changes over time. The degree of browning increases in proportion to the concentration of the amino acid, indicating an apparent first-order reaction

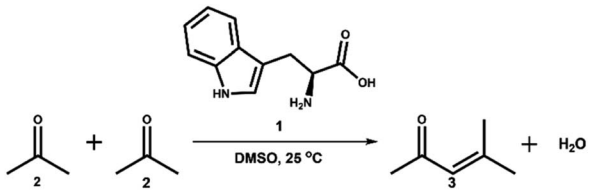

Scheme 1 Self-aldol condensation of acetone (**2**) catalysed by L-tryptophan (**1**) in DMSO solution, leading to the formation of mesityl oxide (MO) (**3**).

with respect to L-tryptophan (Fig. S1†). In our previous investigation, we demonstrated that the extent of L-tryptophan browning is also dependent on the volume fraction of acetone.[9] This underscores the significance of acetone, the simplest and smallest ketone, as a critical reactant resembling the carbonyl compounds involved in the conventional Maillard reaction. However, it is particularly intriguing to observe the reaction between L-tryptophan and acetone in DMSO at room temperature, where no typical catalyst is present. Initially, we propose that acetone undergoes self-aldol condensation, a reaction that conventionally necessitates a strong acid or base catalyst.[32,33] In our specific system utilizing DMSO as the solvent, we hypothesize that L-tryptophan (**1**) facilitates the self-aldol condensation of acetone (**2**), ultimately leading to the formation of MO (**3**), an α,β-unsaturated ketone (Scheme 1).

Fig. S2† depicts a typical HPLC chromatogram that illustrates the identification of an MO peak in the reaction. Consequently, a kinetic study was conducted to measure the concentration–time profiles of MO during the reaction using an HPLC method with diode-array UV detection. This method also enables the simultaneous determination of L-tryptophan and acetone (Table S1 and Fig. S2†).

Fig. 2A illustrates a gradual decomposition of L-tryptophan over a 12 day reaction period under a continuous sampling

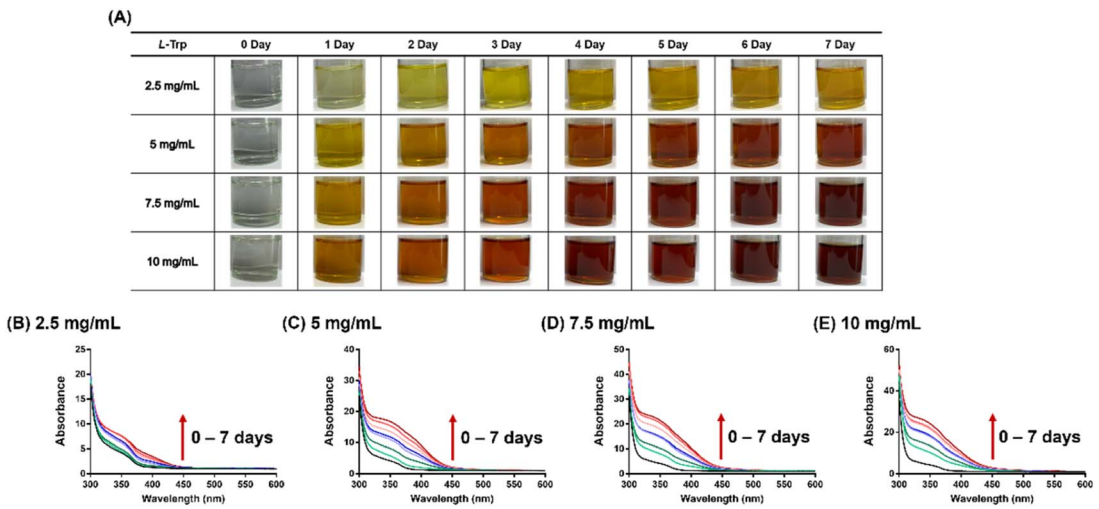

Fig. 1 Browning of L-tryptophan in acetone/DMSO. (A) Visual representation of the browning process. (B–E) UV-Vis spectra (dilution-adjusted absorbance) recorded at different reaction times for solutions containing various concentrations of L-tryptophan in a solvent mixture of 90% v/v DMSO and 10% v/v acetone. The reported absorbance values were adjusted based on the dilution factor.

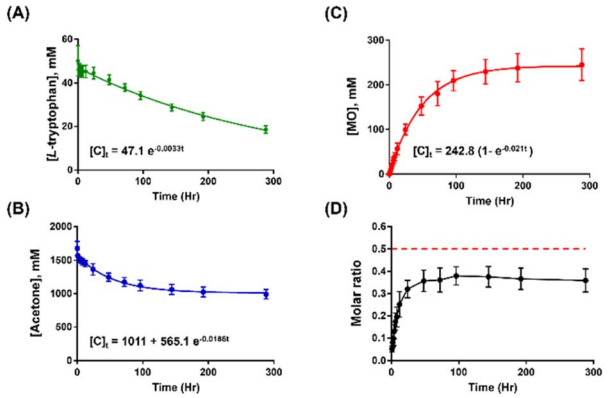

Fig. 2 Chemical kinetics of (A) L-tryptophan, (B) acetone, and (C) MO over 12 days. (D) The molar ratio of formed MO to consumed acetone over 12 days. Red dash line means the theoretical molar ratio is 0.5. All data expressed as means ± SD.

scheme, with the kinetic profile fitting well to first-order kinetics. The estimated half-life for L-tryptophan decomposition is about 9 days. In Fig. 2B, a much faster decline in acetone concentration is observed during the early phase of the reaction, reaching equilibrium after approximately 4 days. The kinetic profile of acetone can be adequately fitted with a first-order kinetics equation, yielding a decomposition rate constant of 0.019 h^{-1}.

Notably, the decomposition kinetics of acetone correspond well to the formation kinetics of MO, as depicted in Fig. 2C. Moreover, the value of the fitted formation rate constant (0.021 h^{-1}) for MO matches the decomposition rate constant of acetone. While acetone is present in large stoichiometric excess compared to L-tryptophan, the kinetic data suggest that L-tryptophan catalyses the activation of acetone, followed by the subsequent condensation of two acetone molecules, leading to the conversion to MO after a dehydration step. This catalytic effect is facilitated by DMSO as the solvent, as the amount of DMSO remained unchanged throughout the course of the reaction (Fig. S3†).

However, it is noteworthy to point out that during the reaction, the molar ratio of formed MO to consumed acetone is increasing over time until reaching a steady-state value of about 0.4 (Fig. 2D). The observation is perplexing because the theoretical molar ratio is 0.5, assuming that 2 acetone molecules form 1 MO molecule. The result suggests that acetone and its derived, activated species are situated in a complex, dynamically changing reaction environment, especially in the very early phase of the reaction where multiple reactive pathways compete with each other, and the more stable brown species are yet to be formed.

At a concentration of 10 mg mL^{-1} (0.34 mol%) of L-tryptophan, the mixed solvent system of acetone and DMSO produces a significant amount of MO (Table 1, entry 1) within 24 hours in a closed reaction system. In this system, the formation of MO increases as the concentration of L-tryptophan rises (Fig. S4†). However, MO is not detected in acetone alone, DMSO alone, or

Table 1 Reactivity of amino acids

Entry	Amino acids[a]	[MO],[b] mM
1	L-Tryptophan	258.1 ± 7.9
2	L-Proline	61.4 ± 9.3
3	L-Phenylalanine	20.8 ± 2.4
4	L-Methionine	9.6 ± 1.1
5	L-Lysine	5.3 ± 0.4
6	L-Serine	1.2 ± 0.1
7	Other amino acids	Trace (<1.2)

[a] Concentration = 10 mg mL^{-1}. [b] Determined after 1 day reaction in a closed reaction system. Data expressed as means ± SD.

the acetone–water mixture (Fig. S5†). These results are consistent with our previous observation that both acetone and DMSO must be present for the browning reaction to occur.[9] The existence of MO in entry 1 was also confirmed through isotope labelling with HR-MS analysis (Fig. S6†).

To further validate our hypothesis regarding acetone's role as a reactant in the production of MO when combined with DMSO and L-tryptophan, we investigated the concentration effect of acetone on MO formation. We examined 5 different concentrations of acetone (5–15% v/v) and analysed the samples by HPLC-DAD for a 3 day reaction at room temperature. The results consistently demonstrated the percentage of acetone consumption (Fig. 3A) and an acetone concentration-dependent increase in MO formation (Fig. 3C) across all experimental groups. Furthermore, we observed a positive correlation between the initial and consumed amounts of acetone (Fig. 3B, $R^2 = 0.858$), as well as between the initial amount of acetone added and the quantity of MO formed (Fig. 3D, $R^2 = 0.910$). The slope value in Fig. 3B indicated that approximately 35% of the acetone was converted to MO, and the ratio of the two slopes

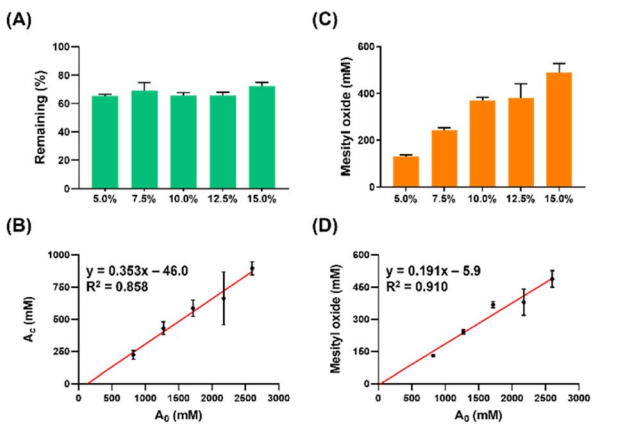

Fig. 3 Acetone consumption and MO formation in the triad reaction system with varied initial amounts of acetone. (A) Percentages of remaining acetone after reacting in different solutions with increasing initial acetone volume percentages. (B) Amount of acetone consumed (A_c) as a function of the initial concentrations of acetone (A_0). (C) Amount of MO formed in each solution. (D) Correlation between MO formation and the initial concentrations of acetone. Means ± SD (n = 3).

(Fig. 3B *vs.* Fig. 3D) suggested that two acetone molecules formed one MO molecule. Additionally, the signal intensity of DMSO remained nearly constant among all groups (Fig. S7†). These findings affirm that the reaction rate is directly proportional to the concentration of acetone, with DMSO serving solely as a facilitator for the self-aldol condensation.

This phenomenon can be explained by the fact that DMSO reduces the stabilization of anions and increases the sensitivity of the system to substituent effect due to its lack of hydrogen-bond donation compared to water.[34] This concept was further supported by the observation that the reactivity of small anions is enhanced when switching from protonic to dipolar aprotic solvents.[35] Besides, in terms of solvation effects, one study reported that acetone forms dihydrogen-bonds in fully aqueous environments but remains non-bonded in fully DMSO solutions.[36] Moreover, polar aprotic solvents leave nucleophiles mostly unprotected, making them more prone to attacking electrophiles.[37] These findings corroborate our hypothesis that the enolate, an anion nucleophile, can more readily attack acetone and form MO due to the lower solvation effect and higher reactivity of anions in DMSO (Fig. S8†).

To assess the reactivity of different amino acids, we also measured the formation of MO for the remaining 19 amino acids (Table 1). L-Proline yields the second-highest amount of MO (entry 2), followed by L-phenylalanine (entry 3), L-methionine (entry 4), L-lysine (entry 5), and L-serine (entry 6). However, the other amino acids exhibit negligible reactivity (entry 7). The partial reactivity of certain amino acids in the reaction system aligns with our previous findings, which demonstrated significant changes over time in the UV-visible spectra of the amino acid solution.[9] Importantly, it should be noted that, except for L-tryptophan, most amino acids show minimal or no potential for browning.[9]

Next, we explored the potential chemical space of the novel browning system using UPLC-TOF-MS. Under optimized LC conditions, the MS scan of the 6 day samples detected over 8000 masses. These were further refined by applying a signal-to-noise ratio threshold of >10, and by excluding early eluted signals, which might represent compounds not subjected to further aldol condensation reactions. From this screening, we extracted the top 30 most intense signals, which are listed in Table S2.† Fig. 4 illustrates the classification of the molecules according to the number of carbon and nitrogen atoms. Notably, the chemical space is enriched with molecules containing 10, 13, 16, 19, and 22 carbon atoms. This finding suggests that L-tryptophan may undergo decarboxylation (–C1), resulting in molecules with 10 carbon atoms, tentatively identified as tryptamine ($C_{10}H_{12}N_2$; Fig. S9†) and indole-3-acetaldehyde ($C_{10}H_9NO$; Fig. S10†). The aldehyde species may further undergo successive aldol condensation reactions with acetone (+C3) or MO (+C6), leading to the formation of molecules with 13, 16, 19, and 22 carbon atoms within this chemical space (Fig. 5).

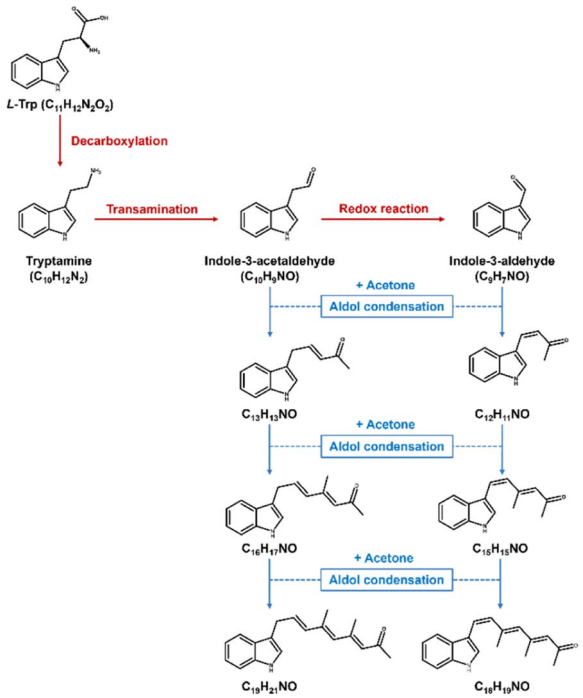

Fig. 5 Possible degradation and aldol condensation reactions between acetone and L-tryptophan.

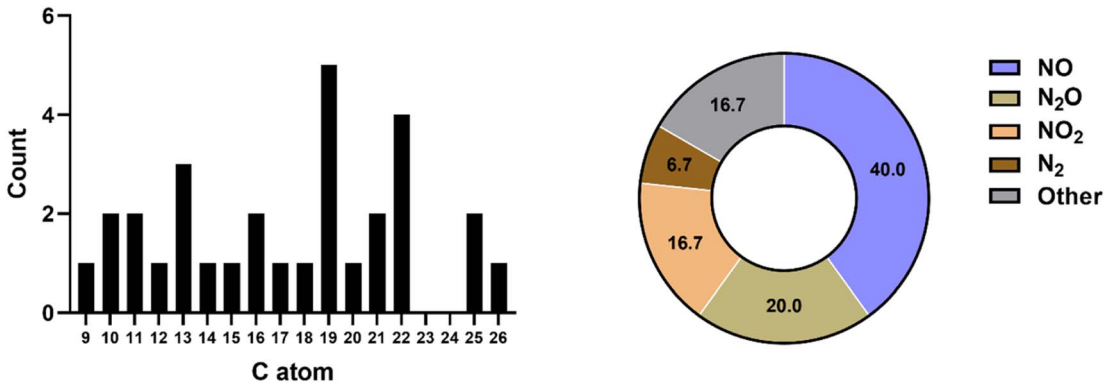

Fig. 4 Distribution of top 30 tentatively assigned molecules in the browning reaction solution of L-tryptophan. (Left) Categorized by the number of carbon atoms; (right) categorized by the number of nitrogen and oxygen atoms.

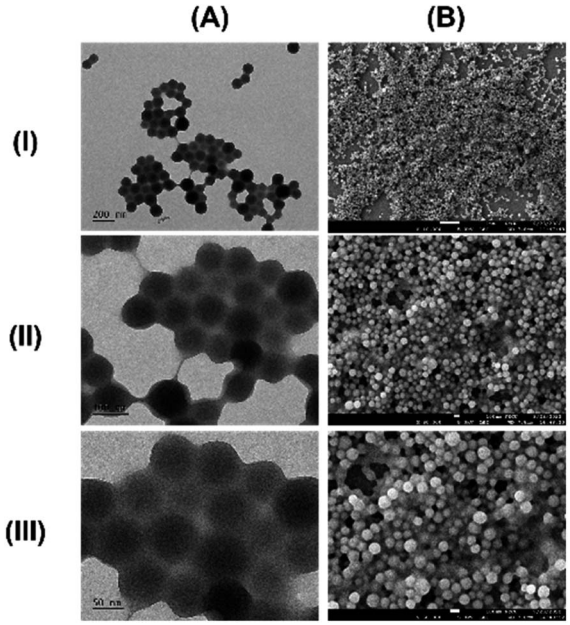

Fig. 6 Electron micrographs of nanoparticles prepared from the browning solution of L-tryptophan. (A) Transmission electron microscopy (TEM); (B) scanning electron microscopy (SEM). Magnifications: (I) 10 000×; (II) 30 000×; (III) 50 000×.

Notably, the reaction system also yields a molecule composed of 9 carbon atoms. We have identified this molecule as most likely being indole-3-aldehyde (C_9H_7NO; Fig. S9†), potentially arising from its precursor through a redox reaction. Aldehydes such as indole-3-aldehyde and indole-3-acetaldehyde can readily engage in aldol condensation with acetone, resulting in the formation of compounds with compositions such as $C_{12}H_{11}NO$, $C_{13}H_{13}NO$, $C_{15}H_{15}NO$, and $C_{16}H_{17}NO$ (Fig. 5). These products may subsequently evolve into compounds with more extensive conjugated systems, like $C_{18}H_{19}NO$ and $C_{19}H_{21}NO$ (Fig. 5), which could conceivably constitute the pigmented compounds within the reaction system. This discovery further substantiates the idea that L-tryptophan may be consumed and transformed into other indole derivatives, subsequently undergoing consecutive aldol condensation reactions with acetone, ultimately leading to the observed browning products.

Finally, we demonstrate that the emerging chemical space encompasses hydrophobic species capable of self-assembling in water through a nanoprecipitation procedure. These brown particles exhibit solid, spherical morphology (Fig. 6) and maintain physical stability in water, with a mean hydrodynamic size of 105 nm (Fig. S11†) and a zeta potential of −15.2 mV. To understand the molecular composition, we extracted the assembled molecules from the purified nanoparticles, followed by analysis using a UPLC-TOF-MS/MS system. The analysis revealed several hydrophobic indole species such as $C_{13}H_{13}NO$, $C_{16}H_{17}NO$, and $C_{18}H_{19}NO$ (Fig. S12†). Consequently, we propose that the assembly mechanism of nanoparticles primarily involves stacking of hydrophobic indole species during the nanoprecipitation process (Fig. 7).

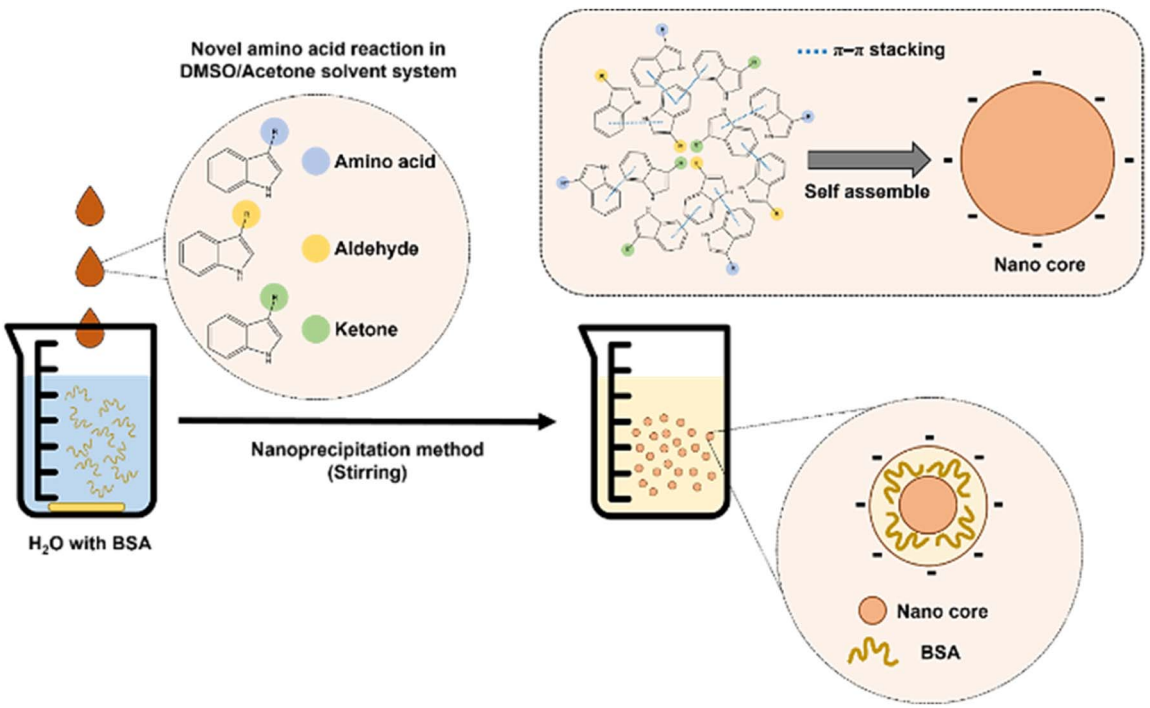

Fig. 7 Schematic representation of the proposed self-assembling process leading to the formation of brown-hued nanoparticles. The browning solution of L-tryptophan in the DMSO/acetone cosolvent was added to water to initiate the nanoparticle formation process. These nanoparticles were effectively stabilized using a 0.01% solution of bovine serum albumin (BSA). The molecular composition of the assembled nanoparticles was determined to consist of various indole derivatives originating from L-tryptophan.

4. Conclusion

In summary, this study aimed to elucidate the chemical processes underlying the browning phenomenon of L-tryptophan within a binary solvent mixture composed of acetone and DMSO. Our investigations have unveiled a dual role played by L-tryptophan within our reaction system. Firstly, it acts as a catalyst, facilitating the direct aldol condensation of acetone and resulting in the formation of a condensed product. Secondly, L-tryptophan functions as a stoichiometric reactant that undergoes consumption and conversion into brown-hued species. Moreover, we have demonstrated that the hydrophobic compounds responsible for the brown color can self-assemble into nanoparticles through a nanoprecipitation mechanism. Subsequent analysis of the prepared nanoparticles has identified their primary constituents as indole derivatives bearing unconjugated side chains. These findings underscore the exciting potential for synthesizing functional nanomaterials with a wide range of applications.

Author contributions

CYH: methodology, investigation, formal analysis, visualization, writing – original draft preparation. HWL: methodology, investigation. TMH: conceptualization, methodology, formal analysis, resources, writing-drafting, reviewing and editing, project administration, supervision.

Conflicts of interest

There are no conflicts to declare.

Acknowledgements

The study was supported by the National Science and Technology Council, Taiwan (MOST 111-2320-B-A49-020-MY3).

References

1 L. C. Maillard, *C. R. Acad. Sci.*, 1912, **154**, 66–68.
2 S. I. Martins, W. M. Jongen and M. A. Van Boekel, *Trends Food Sci. Technol.*, 2000, **11**, 364–373.
3 M. Murata, *Glycoconjugate J.*, 2021, **38**, 283–292.
4 A. Shakoor, C. Zhang, J. Xie and X. Yang, *Food Chem.*, 2022, **393**, 133416.
5 S. Affes, R. Nasri, S. Li, T. Thami, A. van Der Lee, M. Nasri and H. Maalej, *Carbohydr. Polym.*, 2021, **255**, 117341.
6 F. Wang, H. Shen, X. Yang, T. Liu, Y. Yang, X. Zhou, P. Zhao and Y. Guo, *RSC Adv.*, 2021, **11**, 27772–27781.
7 J. Cao, H. Yan and L. Liu, *LWT*, 2022, **161**, 113343.
8 D. D. Kitts, *Antioxidants*, 2021, **10**, 1840.
9 T.-M. Hu and Y.-H. Chiang, *Biochem. Biophys. Res. Commun.*, 2021, **536**, 67–72.
10 B. List, R. A. Lerner and C. F. Barbas, *J. Am. Chem. Soc.*, 2000, **122**, 2395–2396.
11 S. Bahmanyar and K. Houk, *J. Am. Chem. Soc.*, 2001, **123**, 12911–12912.
12 S. Bahmanyar and K. Houk, *J. Am. Chem. Soc.*, 2001, **123**, 11273–11283.
13 L. Hoang, S. Bahmanyar, K. Houk and B. List, *J. Am. Chem. Soc.*, 2003, **125**, 16–17.
14 B. List, L. Hoang and H. J. Martin, *Proc. Natl. Acad. Sci.*, 2004, **101**, 5839–5842.
15 A. Córdova, W. Zou, I. Ibrahem, E. Reyes, M. Engqvist and W.-W. Liao, *Chem. Commun.*, 2005, 3586–3588.
16 B. M. Trost and C. S. Brindle, *Chem. Soc. Rev.*, 2010, **39**, 1600–1632.
17 M. Abuaf, S. Das and Y. Mastai, *RSC Adv.*, 2023, **13**, 1580–1586.
18 L. Claes, M. Janssen and D. E. De Vos, *ChemCatChem*, 2019, **11**, 4297–4306.
19 B. Borah, K. D. Dwivedi and L. R. Chowhan, *RSC Adv.*, 2021, **11**, 13585–13601.
20 A. Katsnelson, *ACS Cent. Sci.*, 2020, **6**, 1854–1857.
21 G. E. Arnold, L. A. Day and A. K. Dunker, *Biochemistry*, 1992, **31**, 7948–7956.
22 Z. Jiang, Z. Liang, X. Wu and Y. Lu, *Chem. Commun.*, 2006, 2801–2803.
23 M. Raj and V. K. Singh, *Chem. Commun.*, 2009, 6687–6703.
24 M. Wang, Y. Jin, J. Li and C.-T. Ho, *J. Agric. Food Chem.*, 1999, **47**, 48–50.
25 B. Rönner, H. Lerche, W. Bergmüller, C. Freilinger, T. Severin and M. Pischetsrieder, *J. Agric. Food Chem.*, 2000, **48**, 2111–2116.
26 S. Diem and M. Herderich, *J. Agric. Food Chem.*, 2001, **49**, 2486–2492.
27 T. Herraiz, A. Peña and A. Salgado, *J. Agric. Food Chem.*, 2023, **71**, 13451–13461.
28 C. Nagai, K. Noda, A. Kirihara, Y. Tomita and M. Murata, *Food Sci. Technol. Res.*, 2019, **25**, 81–88.
29 S. H. Lee, S. J. Jeong, G. Y. Jang, M. Y. Kim, I. G. Hwang, H. Y. Kim, K. S. Woo, B. Y. Hwang, J. Song and J. Lee, *J. Agric. Food Chem.*, 2016, **64**, 3041–3047.
30 D. Qin, L. Li, J. Li, J. Li, D. Zhao, Y. Li, B. Li and X. Zhang, *J. Agric. Food Chem.*, 2018, **66**, 6752–6761.
31 S. Bellmaine, A. Schnellbaecher and A. Zimmer, *Free Radicals Biol. Med.*, 2020, **160**, 696–718.
32 N. Lorette, *J. Org. Chem.*, 1957, **22**, 346–347.
33 A. T. Nielsen and W. J. Houlihan, *Org. React.*, 2004, **16**, 1–438.
34 D. L. Hughes, J. J. Bergan and E. J. J. Grabowski, *J. Org. Chem.*, 1986, **51**, 2579–2585.
35 D. Martin, A. Weise and H.-J. Niclas, *Angew Chem. Int. Ed. Engl.*, 1967, **6**, 318–334.
36 M. C. R. Symons and G. Eaton, *J. Chem. Soc., Faraday Trans. 1*, 1985, **81**, 1963–1977.
37 A. J. Parker, *Chem. Rev.*, 1969, **69**, 1–32.